Magnetic Phase Diagram and Transport Properties of the *t-J* Model: A Spin-Rotation-Invariant Slave-Boson Approach

1994 Europhys. Lett. 26 109

(http://iopscience.iop.org/0295-5075/26/2/006)

EUROPHYSICS LETTERS 10 April 1994

Europhys. Lett., **26** (2), pp. 109-115 (1994)

Magnetic Phase Diagram and Transport Properties of the *t-J* Model: a Spin-Rotation–Invariant Slave-Boson Approach.

M. DEEG, H. FEHSKE and H. BÜTTNER

Physikalisches Institut, Universität Bayreuth - D-95440 Bayreuth, Germany

(received 30 July 1993; accepted in final form 7 February 1994)

PACS. 71.28 – Narrow-band systems, heavy-fermion metals: intermediate-valence solids.
PACS. 71.45G – Exchange, correlation, dielectric and magnetic functions, plasmons.
PACS. 75.10 – General theory and models of magnetic ordering.

Abstract. – On the basis of a spin-rotation–invariant formulation of the Kotliar-Ruckenstein slave-boson representation the *t-J* model is studied on a square lattice. The ground-state phase diagram is derived numerically, by taking into account also incommensurate magnetic structures. The domain of phase separation is determined. The correlation-induced band renormalization is in excellent agreement with Lanczos results. We calculated the doping dependence of Hall resistivity and thermopower using the relaxation time approximation, the results being in accord with experiments on $La_{2-\delta}Sr_{\delta}CuO_4$.

The unusual normal-state properties are some of the most interesting features of the high-temperature superconductors (*e.g.* Hall coefficient [1], thermopower [2], spin dynamics in the metallic state [3]). The strong electronic correlations in the CuO_2 planes, which are commonly believed to be responsible for these effects, may be described by «simple» two-dimensional (2D) models like the *t-J*, Hubbard or Emery model.

For the theoretical investigation of the *t-J* model slave-field techniques [4, 5] are of increasing importance. Within the scope of slave-fermion mean-field theories, the magnetic ground-state phase diagram of the *t-J* model shows antiferro- (AFM), ferro- (FM), and para-magnetic (PM) as well as incommensurate spiral order [5], and at low doping and large J an instability towards phase separation. However, the *mean-field* slave-fermion schemes suffer from neglecting important correlation effects, especially the fermion charge degrees of freedom are not described sufficiently well [6]. In contrast, the slave-boson (SB) saddle-point approximation, introduced by Kotliar and Ruckenstein [7] for the Hubbard model, treats spin and charge degrees of freedom on an equal footing. By including spiral magnetic states, the phase diagram for the large-U Hubbard model was determined within a spin-rotation–invariant extension [8] of this theory [9]. To treat the strong AFM exchange, Kaga [10] included SB fluctuations via a loop expansion in the functional integral. The effective *t-J* Lagrangian, derived in this way, contains only an Ising interaction term, spin-flip exchange processes are neglected. To bosonize the complete exchange interaction term of the *t-J* model, one has to use the spin-rotation–invariant formulation of the Kotliar-Ruckenstein SB approach (SRI SB) [6].

Transport coefficients of the Hubbard strong-coupling model have been calculated by Trugman [11]. Based on an exact treatment of this model in a variational space, an effective quasi-particle band is derived to obtain the transport coefficients within rigid-band and relaxation time approximation, where the incorporation of correlation effects yields a qualitative agreement with experiment. In contrast, the transport properties of the t-t'-J model, calculated by Chi and Nagi [12], result from a simple band dispersion effect, depending on the next-nearest-neighbour hopping t'. In ref. [12], the quasi-particle band was determined in the $J = 0$ limit, using the SB theory of Zou and Anderson [4]. Sá de Melo *et al.* [13] showed that a systematic treatment of the strong AFM correlations within the spinon holon picture leads to $\boldsymbol{k}$-dependent corrections of the quasi-particle self-energy. This effect is sufficient to reproduce the experimentally observed sign change in the Hall coefficient. So far there exist no *consistent* calculations of the transport properties within the Kotliar-Ruckenstein SB approach.

In this paper, we present the magnetic phase diagram of the t-J model within the SRI SB saddle-point approximation, including AFM, FM and PM as well as incommensurate spiral order. We discuss the existence of phase separation and calculate Hall resistivity and thermopower within the relaxation time approach, taking the self-consistent quasi-particle band from the SRI SB approach as input. In addition, we apply the Trugman procedure [11] to the rigid (coherent) band obtained from exact diagonalization (ED) on finite lattices [14]. Finally, we compare our results with $La_{2-\delta}Sr_{\delta}CuO_4$ experiments.

The starting point of our theoretical work is the 2D t-J model

$$\mathcal{H}_{t\text{-}J} = -t \sum_{\langle ij \rangle,\,\sigma} (\tilde{c}_{i\sigma}^{\dagger} \tilde{c}_{j\sigma} + \text{h.c.}) + J \sum_{\langle ij \rangle} \left(\boldsymbol{S}_i \cdot \boldsymbol{S}_j - \frac{n_i n_j}{4} \right), \tag{1}$$

on a square lattice in standard notation. In the SRI SB theory the Hilbert space is enlarged by introducing auxiliary boson fields $e_i^{(\dagger)}$ and matrix operators $\underline{p}_i^{(\dagger)}$, representing empty sites ($|0\rangle = e^{\dagger}|\text{vac}\rangle$), and single occupied sites with spin-projection $\sigma(|\sigma\rangle = \sum_{\rho} f_{\rho}^{\dagger} p_{\rho\sigma}^{\dagger} |\text{vac}\rangle)$, respectively. $\underline{p}^{(\dagger)} = (1/2) \sum_{\mu} \underline{\tau}_{\mu} p_{\mu}^{(\dagger)}$ is expressed in terms of the scalar field $p_0^{(\dagger)}$ and the vector field $\boldsymbol{p}^{(\dagger)}$, where $\underline{\tau}_{\mu}$ denote the Pauli matrices. The operators $p_{\mu}^{(\dagger)}$ ($\mu = 0, x, y, z$) satisfy bosonic commutation rules. The pseudofermions $f_{\rho}^{\dagger}$ are components of the spinor $\Psi^{\dagger} = (f_{+}^{\dagger}, f_{-}^{\dagger})$. Consequently, in this representation the state $|\sigma\rangle$ transforms as a spinor and the spin-rotation invariance is ensured. The electron number n_i is given by $n_i = \Psi_i^{\dagger} \Psi_i$, *i.e.* the one-to-one correspondence of the Fermi-liquid concept is fulfilled. To eliminate unphysical states in the extended Hilbert space, the SB fields have to satisfy local constraints:

$$C^{(1)} = e^{\dagger} e + \sum_{\mu} p_{\mu}^{\dagger} p_{\mu} - 1 = 0 \quad \text{(completeness)}, \tag{2}$$

$$C_{\rho\bar{\rho}}^{(2)} = f_{\rho}^{\dagger} f_{\bar{\rho}} - 2 \sum_{\rho'} p_{\bar{\rho}\rho'}^{\dagger} p_{\rho'\rho} = 0 \quad \text{(SB correspondence)}. \tag{3}$$

The electron annihilation operator is replaced by $\tilde{c}_{i\sigma} = \sum_{\rho} z_{i\sigma\rho} f_{i\rho}$, where $\underline{z} = \underline{L} e^{\dagger} M \underline{p} \underline{R}$, with the renormalization factors $\underline{R} = [(1 - e^{\dagger} e) \underline{1} - 2 \underline{\tilde{p}}^{\dagger} \underline{\tilde{p}}]^{-1/2}$, $\underline{L} = [\underline{1} - 2 \underline{p}^{\dagger} \underline{p}]^{-1/2}$, $M = [1 + e^{\dagger} e + 2\,\text{Tr}\, \underline{p}^{\dagger} \underline{p}]^{1/2}$, and $\tilde{p}_{\rho\rho'}^{(\dagger)} := \rho\rho' p_{-\rho',-\rho}^{(\dagger)}$ [6]. Then the transformed Hamiltonian reads as

$$\mathcal{H}_{t\text{-}J}^{\text{SB}} = -t \sum_{\langle ij \rangle} \Psi_i^{\dagger} \underline{z}_i^{\dagger} \underline{z}_j \Psi_j + \text{h.c.} + J \sum_{\langle ij \rangle} \left(\boldsymbol{S}_i (p_{i\mu}) \cdot \boldsymbol{S}_j (p_{j\mu}) - \frac{n_i (p_{i\mu}) n_j (p_{j\mu})}{4} \right), \tag{4}$$

where in the bosonized interaction term the electron density and the spin are expressed by the boson operators:

$$n_i(p_{i\mu}) = 2\,\mathrm{Tr}\,\underline{p}^\dagger \underline{p} = \sum_\mu p_{i\mu}^\dagger p_{i\mu}\,, \tag{5}$$

$$\boldsymbol{S}_i(p_{i\mu}) = \mathrm{Tr}\,\underline{p}_i^\dagger\, \underline{\boldsymbol{\tau}}\, \underline{p}_i = \frac{1}{2}\,(p_{i0}^\dagger \boldsymbol{p}_i + \boldsymbol{p}_i^\dagger p_{i0} - i\boldsymbol{p}_i^\dagger \times \boldsymbol{p}_i)\,. \tag{6}$$

The constraints are ensured by introducing the Lagrange multipliers $\lambda^{(1)}$ and $\lambda_\mu^{(2)}$, *i.e.* $\mathscr{H}_{t\text{-}J}^{\mathrm{SB}} \to \mathscr{H}_{t\text{-}J}^{\mathrm{SB}} + \sum_i (C_i^{(1)}\lambda_i^{(1)} + \mathrm{Tr}\,\underline{C}_i^{(2)}\underline{\lambda}_i^{(2)})$, with $\underline{\lambda}_i^{(2)} = \sum_\mu \underline{\tau}_\mu \lambda_{i\mu}^{(2)}$. Note that additional constraints do not exist (1). $\boldsymbol{S}_i(p_{i\mu})$ (6) satisfies the spin algebra and, if the constraints (2, 3) are fulfilled, $\mathscr{H}_{t\text{-}J}^{\mathrm{SB}}$ yields the same matrix elements as the original Hamiltonian (1). Thus the SRI SB representation is equivalent to the usual fermionic representation of the *t-J* model. Let us emphasize that in the scalar KR representation the matrix elements of the interaction term are not reproduced. Thus the SRI SB scheme (2)-(6) provides a consistent bosonization of the *t-J* model.

To proceed, the partition function is expressed by a coherent-state imaginary time path integral over complex boson and pseudofermion Grassmann fields. Then the resulting Lagrangian is invariant under a local $SU(2) \otimes U(1)$ gauge transformation: $\underline{p}_i \to \underline{p}_i \exp[-i\underline{\chi}_i]$, $e_i \to e_i \exp[-i\underline{\theta}_i]$, and $\Psi_i \to \exp[-i\theta_i]\exp[i\underline{\chi}_i]\Psi_i$. The Lagrange multipliers, which act as gauge fields, are transformed as $\underline{\lambda}_i^{(2)} \to \exp[i\underline{\chi}_i]\underline{\lambda}_i^{(2)}\exp[-i\underline{\chi}_i] - i\dot{\underline{\chi}}_i + i\dot{\theta}_i \underline{1}$, and $\lambda_i^{(1)} \to \lambda_i^{(1)} + i\dot{\theta}_i$, *i.e.* they become dynamic. The gauge invariance of the Lagrangian can be used to remove five phases in the so-called radial gauge. As a consequence all SB fields become real, in contrast to the Hubbard model, where one SB field remains complex [6, 15]. Finally, the fermionic degrees of freedom are integrated out exactly. It should be emphasized that the interaction term is now completely represented by *real* boson fields.

This bosonized action is treated within the saddle-point approximation. To keep the problem tractable, we use the ansatz $\boldsymbol{m}_i \propto \hat{n}_i = (\cos \boldsymbol{Q}\cdot\boldsymbol{R}_i, \sin\boldsymbol{Q}\cdot\boldsymbol{R}_i, 0)$ for the local magnetization, which is given as $\boldsymbol{m}_i = -2\boldsymbol{S}_i = -2p_{i0}\boldsymbol{p}_i$. Thereby, a new «variational parameter» $\boldsymbol{Q}$ is introduced to describe several magnetic ordered states: PM, FM [$\boldsymbol{Q} = 0$], AFM [$\boldsymbol{Q} = (\pi, \pi)$], and incommensurate (1, 1)-spiral [$\boldsymbol{Q} = (Q, Q)$], (1, 0)-spiral [$\boldsymbol{Q} = (Q, \pi)$], and (0, Q)-spiral [$\boldsymbol{Q} = (0, Q)$] states. Note that since fluctuations of the charge density are not incorporated, the scalar bosons are homogeneous: $e_i = e$, $p_{i0} = p_0$, $\lambda_i^{(1)} = \lambda^{(1)}$, and $\lambda_{i0}^{(2)} = \lambda_0$. The vector fields exhibit the same spatial variation as the magnetization: $\boldsymbol{p}_i = p\hat{n}_i$ and $\boldsymbol{\lambda}_i^{(2)} = \lambda\hat{n}_i$.

Then the free energy per site is given by

$$f_{t\text{-}J}^{\mathrm{SB}} = \lambda^{(1)}(e^2 + p_0^2 + p^2 - 1) - \lambda_0(p_0^2 + p^2) - 2\lambda p_0 p + \mu n + $$
$$+ J\left[p_0^2 p^2(\cos Q_x + \cos Q_y) - \frac{1}{2}(p_0^2 + p^2)^2\right] - \frac{1}{\beta N}\sum_{k\nu} \ln\{1 + \exp[-\beta(E_{k\nu} - \mu)]\}\,. \tag{7}$$

$$E_{k\nu} = \frac{1}{2}(z_+^2 + z_-^2)(\varepsilon_{\boldsymbol{k}} + \varepsilon_{\boldsymbol{k}-\boldsymbol{Q}}) + \lambda_0 + $$
$$+ \nu\frac{1}{2}[(z_+^2 - z_-^2)^2(\varepsilon_{\boldsymbol{k}} - \varepsilon_{\boldsymbol{k}-\boldsymbol{Q}})^2 + 4(z_+ z_-(\varepsilon_{\boldsymbol{k}} + \varepsilon_{\boldsymbol{k}-\boldsymbol{Q}}) + \lambda)^2]^{1/2}$$

(1) Especially, if the constraint $\boldsymbol{p}^\dagger \times \boldsymbol{p} = 0$ is added [6], the spin algebra is not satisfied.

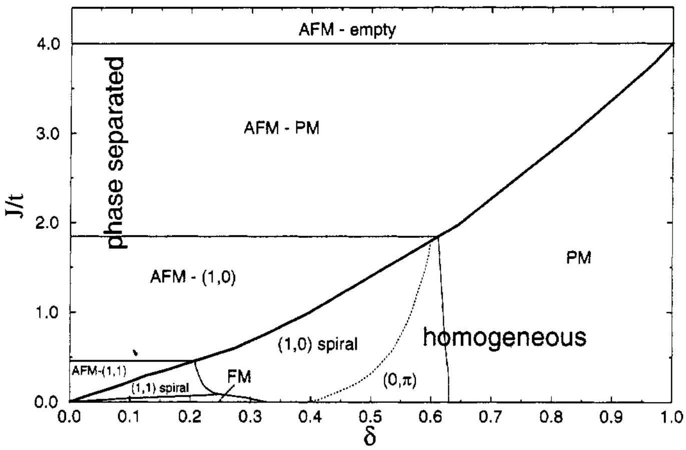

Fig. 1. - SB ground-state phase diagram of the t-J model.

denote the quasi-particle energies, where $z_\pm = z_1 \pm z_2$ are obtained from the eigenvalues of $\underline{z}$, and $\varepsilon_k = -2t(\cos k_x + \cos k_y)$. To determine the stationary points of the action, the free energy is minimized with respect to the boson fields, the Lagrange multipliers and the wave vector $\boldsymbol{Q}$, leading to a system of non-linear saddle-point equations, which is solved numerically.

The resulting ground-state phase diagram in the (J, δ)-plane (doping $\delta = 1 - n$) is shown in fig. 1. For the case $\delta = 0$ (Heisenberg model), we obtain an AFM ground state. For $J = 0$, the FM is lowest in energy up to a hole concentration of 0.327, where a first-order transition to the $(1, 0)$-spiral takes place; above $\delta = 0.39$, we find a degenerate ground state with wave vector $(0, \pi)$. At $\delta = 0.63$ the PM is the lowest in energy state (second-order transition). This coincides with the $U \to \infty$ SB results of the Hubbard model ($J = 4t^2/U$), given in [9]. The PM-FM instability occurs at $\delta_{\text{PM-FM}} = 0.33$ [15]. In contrast, the slave-fermion phase diagram [5] exhibits a much larger FM region. This can be taken as an indication that correlation effects are treated less accurately within the slave-fermion mean-field scheme [5].

For finite exchange interaction J the $(1, 1)$-spiral is the ground state at small doping. With increasing δ a transition to the FM takes place, which becomes unstable against the $(1, 0)$-spiral at larger doping concentrations. For $J/t > 0.08$, we find a transition from $(1, 1)$- to $(1, 0)$-spirals at about $\delta \approx 0.2$. In fig. 1, the dotted line separates the $(1, 0)$-spiral state from the region, where the $(1, 0)$ and $(0, \pi)$ states are degenerate. To investigate the widely debated instability towards phase separation into hole-rich and AFM regions (which is related to a concave curvature of the free energy as a function of δ), the domain of inhomogeneous states is determined by a Maxwell construction. This two-phase region consists of the phase without holes, which is AFM ordered, and the corresponding hole-rich state on the right boundary of the respective region. At $J = 0$ (cf. the $U \to \infty$ in [15]), the free energy is a convex function $\forall \delta$, *i.e.* our SRI SB theory does not support recent arguments [16] for phase separation in this limit. For $J/t > J_{\text{PS}}/t = 4.0$ *complete* charge separation takes place, an essentially classical result. From ED we obtain $J_{\text{PS}}/t = 4.1(\pm 0.1)$ [17], to be compared with $J_{\text{PS}}/t = 3.8$ derived by means of a high-temperature expansion [18]. The line separating the two-phase region from the stable states was determined by Marder *et al.* [19] within a semi-classical theory to vary as $J/t = 4\delta^2$, whereas our theory yields an approximately linear dependence at small δ. We believe that, due to an

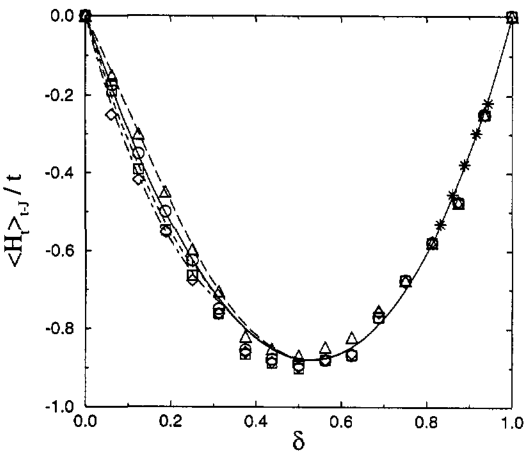

Fig. 2.

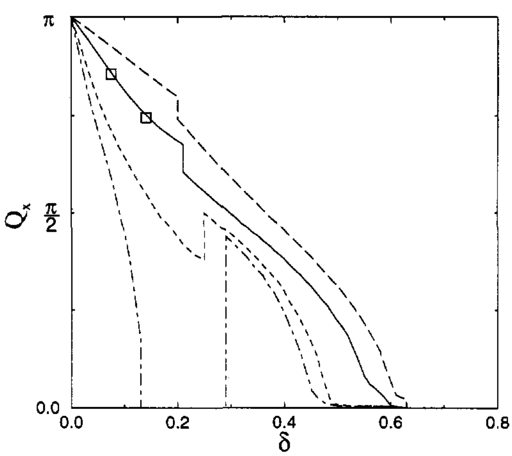

Fig. 3.

Fig. 2. – Expectation value of the kinetic energy as a function of doping at several interaction strengths J in comparison to ED results for 16 (36) site lattice [14, 17]. (--- SB ($J/t = 1.0$), △ ED 16 ($J/t = 1.0$), —— SB ($J/t = 0.4$), ○ ED 16 ($J/t = 0.4$), ---- SB ($J/t = 0.1$), □ ED 16 ($J/t = 0.1$), ---- SB ($J/t = 0.0$), ◇ ED 16 ($J/t = 0.0$), * ED 16 ($J/t = 0.0$).)

Fig. 3. – The x-component of the spiral wave vector $\boldsymbol{Q}$ as a function of doping compared with experiment [3]. (□ experiment (Sr), --- SB ($J/t = 1.0$), —— SB ($J/t = 0.4$), ---- SB ($J/t = 0.1$), ---- SB ($J/t = 0.05$).)

improved treatment of spin fluctuations in our approach, the region of *uncomplete* phase separation is reduced. The instability towards phase separation at small J can be taken as an indication that charge fluctuations may play an important role as well. Let us emphasize that Puttika *et al.* [18] obtained a critical exchange $J/t = 1.2$ for phase separation as $\delta \to 0$, a result which is not confirmed by the present as well as different approaches [16, 19, 20] (cf. fig. 1*b*) in [20]).

The expectation value of the kinetic energy is compared with the result from ED for a finite 16-site [14] (36-site [17]) lattice in fig. 2. There is excellent agreement between SB results and ED data. Obviously, this result does not depend on the interaction strength J, *i.e.* the SB theory well describes the correlation effects. $\langle \mathcal{H}_t \rangle_{t\text{-}J}/t$ is directly related to the effective transfer amplitude of the renormalized quasi-particle band, which is taken as input for the calculation of transport coefficients.

The x-component of the spiral wave vector $\boldsymbol{Q}$ is shown as a function of doping in fig. 3. At $\delta = 0$, $\boldsymbol{Q} = (\pi, \pi)$ indicates the AFM order. At low doping the (1, 1)-spiral order vector decreases approximately linearly. With decreasing J the AFM exchange is weakened, consequently the deviation of the order vector from (π, π) increases. The discontinuities reflect the first-order transition from (1, 1)- to (1, 0)-spirals. For $J/t = 0.05$ the transition to the FM takes place, with Q_x jumping down to zero. The (1, 0)-spiral wave vector shows a monotonous decrease of Q_x until at $\delta = 0.63$ the transition to the PM ($Q_x = 0$) occurs. Comparing the magnitude of the theoretical order vector of the spiral solutions to results from inelastic-neutron-scattering experiments on $La_{2-\delta}Sr_\delta CuO_4$ [3], we find good agreement for an exchange interaction strength of $J/t = 0.4$ (which seems to be a reasonable value with respect to the strong electron correlations observed in the high T_c's).

The self-consistent renormalized SB quasi-particle band is now taken to calculate the

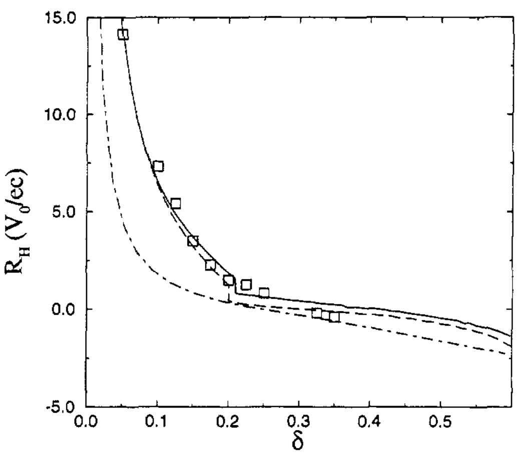

Fig. 4.

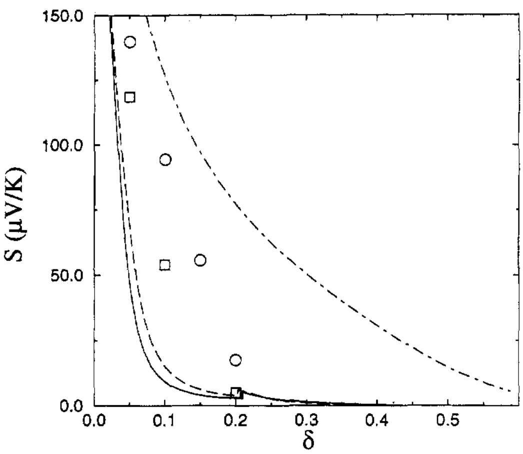

Fig. 5.

Fig. 4. – Hall resistivity R_H at 80 K as a function of doping. The SB results are compared with ED and experiment [1], where t is fixed to 0.3 eV. (□ experiment (Sr), ---- ED t-J($J/t = 0.4$), —— SB t-J ($J/t = 0.4$), --- SB t-J ($J/t = 1.0$).)

Fig. 5. – Thermopower S at 300 K as a function of doping. The SB results are compared with ED and experiment [2]. (□ experiment (Sr), ○ experiment (Ba), ---- ED t-J($J/t = 0.4$), —— SB t-J ($J/t = 0.4$), --- SB t-J ($J/t = 1.0$).)

transport properties. The Hall resistivity R_H and the thermopower S are given by $R_H = \sigma_{xyz}/\sigma_{xx}\sigma_{yy}$ and $S_{\alpha\beta} = -(\sigma)^{-1}_{\alpha\gamma}\nu_{\gamma\beta}$, respectively, where the transport coefficients $\sigma_{\alpha\beta\gamma}$, $\sigma_{\alpha\beta}$ and $\nu_{\alpha\beta}$ are obtained within relaxation time approximation by the standard Brillouin-zone integrals. Note that we only calculate properties which are independent of the relaxation time, because we are not able to determine this quantity.

The Hall resistivity at a temperature of 80 K is shown in fig. 4 together with the experimental data of Takagi *et al.* [1]. The agreement between the experiment and the theoretical SB values is surprisingly good. For small doping the structure of the Fermi surface yields to a holelike sign of R_H. The change of sign, as experimentally observed at about $\delta \approx 0.3$, occurs at $\delta \approx 0.4$ ($\delta \approx 0.3$) for $J/t = 0.4$ ($J/t = 1.0$). The results calculated with the rigid band from ED agree qualitatively with the experiment, as well as the results of Trugman [11].

Finally the thermopower is shown in fig. 5. Of course, compared to the high experimental temperature (300 K) the saddle-point approximation is expected to be less accurate. However, it seems that the agreement with the experiment of Cooper *et al.* [2] again is surprisingly good, at least qualitatively.

In summary, we applied the SRI SB theory to the t-J model and mapped out, to our knowledge for the first time, the magnetic ground-state phase diagram, including incommensurate magnetic structures. We investigated the stability of the phases and determined the region of phase separation. The self-consistent band renormalization by the correlations is in excellent agreement compared with exact diagonalization. The spiral order vector and the Hall resistivity agree very well with the experimental values at low temperatures for an exchange interaction $J/t = 0.4$.

* * *

We would like to thank D. IHLE, A. MURAMATSU and W. ZIEGLER for helpful discussions and K. FESSER for a critical reading of the manuscript. The authors also thank the referee for useful comments.

REFERENCES

[1] TAKAGI T. *et al.*, *Phys. Rev. B*, 40 (1989) 2254.
[2] COOPER J. R. *et al.*, *Phys. Rev. B*, **35** (1987) 8794.
[3] CHEONG S.-W. *et al.*, *Phys. Rev. Lett.*, **67** (1991) 1791.
[4] ZOU Z. and ANDERSON P. W., *Phys. Rev. B*, **37** (1988) 627.
[5] SARKER S. K., *Phys. Rev. B*, **47** (1993) 2940.
[6] FRÉSARD R. and WÖLFLE P., *Int. J. Mod. Phys. B*, **6** (1992) 685; 3087(E).
[7] KOTLIAR G. and RUCKENSTEIN A. E., *Phys. Rev. Lett.*, **57** (1986) 1362.
[8] LI T., WÖLFLE P. and HIRSCHFELD P. J., *Phys. Rev. B*, **40** (1989) 6817.
[9] MÖLLER B., DOLL K. and FRÉSARD R., *J. Phys. Condens. Matter*, **5** (1993) 4847.
[10] KAGA H., *Phys. Rev. B*, **46** (1992) 1979.
[11] TRUGMAN S. A., *Phys. Rev. Lett.*, **65** (1990) 500.
[12] CHI H. and NAGI A. D. S., *Phys. Rev. B*, **46** (1992) 421.
[13] SÁ DE MELO C. A. R., WANG Z. and DONIACH S., *Phys. Rev. Lett.*, 68 (1992) 2078.
[14] FEHSKE H., WAAS V., RÖDER H. and BÜTTNER H., *Phys. Rev. B*, **44** (1991) 8473.
[15] DEEG M., FEHSKE H. and BÜTTNER H., *Z. Phys. B*, **88** (1992) 283.
[16] EMERY V. J., KIVELSON S. A. and LIN H. Q., *Phys. Rev. Lett.*, **64** (1990) 475.
[17] WAAS V., FEHSKE H. and BÜTTNER H., *Phys. Rev. B*, 48 (1993) 9106.
[18] PUTTIKA W. O., LUCHINI M. and RICE T. M., *Phys. Rev. Lett.*, **68** (1992) 538.
[19] MARDER M., PAPANICOLAOU N. and PSALTAKIS G. C., *Phys. Rev. B*, **41**(1990) 6920.
[20] DE MELLO E. V. L., *J. Phys. Condens. Matter*, **6** (1994) 117.